

Seamless Routing and Cooperative Localization of Multiple Mobile Robots for Search and Rescue Application

Chang-Eun Lee, Hyun-Ja Im, Jeong-Min Lim, Young-Jo Cho and Tae-Kyung Sung

In particular, for a practical mobile robot team to perform such a task as that of carrying out a search and rescue mission in a disaster area, the network connectivity and localization have to be guaranteed even in an environment where the network infrastructure is destroyed or a Global Positioning System is unavailable. This paper proposes the new collective intelligence network management architecture of multiple mobile robots supporting seamless network connectivity and cooperative localization. The proposed architecture includes a resource manager that makes the robots move around and not disconnect from the network link by considering the strength of the network signal and link quality. The location manager in the architecture supports localizing robots seamlessly by finding the relative locations of the robots as they move from a global outdoor environment to a local indoor position. The proposed schemes assuring network connectivity and localization were validated through numerical simulations and applied to a search and rescue robot team.

Keywords: Network connectivity and localization, seamless routing, cooperative localization, global positioning system, resource manager, location manager, CINEMA.

Manuscript received Aug. 10, 2014; revised Dec. 11, 2014; accepted Dec. 26, 2014.

This work was supported by the Industrial Foundation Technology Development Program of MKE/KEIT [Development of Collective Intelligence Robot Technologies].

Chang-Eun Lee (corresponding author, celee@etri.re.kr), Hyun-Ja Im (mm27@etri.re.kr), and Young-Jo Cho (youngjo@etri.re.kr) are with the IT Convergence Technology Research Laboratory, ETRI, Daejeon, Rep. of Korea.

Jeong-Min Lim (likebasic@naver.com) and Tae-Kyung Sung (tksaint@cnu.ac.kr) are with the Department of Information and Communication Engineering, Chungnam National University, Daejeon, Rep. of Korea.

I. Introduction

Multiple cooperative mobile robots performing search and rescue missions in disaster areas always require communication links to the human operator located at a remote station. However, the network infrastructure constructing the communication link is often destroyed in disaster areas; thus, a multi-hop mesh network connecting all robots and the operator station is needed for maintaining the link connectivity. In a multi-hop mesh network where the link environment is poor, the network configuration and routing of mobile robots are very important issues to guarantee the quality of service (QoS) of the communication link.

Addressing these issues, J. Fink and others [1]–[2] proposed a k -connectivity method and resolved the end-to-end network connectivity problem using a probabilistic approach. In the DARPA LANdroids project [3], a self-configuring network scheme was developed, where the global network connectivity is maintained even in the case of a local connection failure. L. Sabattini and others [4]; S. Zickler and M. Veloso [5]; M.M. Zavlanos and others [6]; and N. Bezzo and others [7] analyzed the graph theoretical connectivity in mobile robot networks and developed optimization-based connectivity control methods. However, most previous approaches assumed that the network was connected within a fixed range of communication and that it relied on direct line-of-sight signals. Moreover, they used only the distance data between robots, which may not reflect the network connection information reasonably. In indoor or dynamic environments, a multi-path problem typically occurs; thus, the range information may become irregular. Therefore,

the network connection might fail in a real environment.

On the other hand, while the mobile robots are monitored and controlled by the remote operator station, it is important to know their locations. In real environments such as disaster areas, however, a GPS is often unavailable and an alternative localization method is required for multiple robots to perform a search and rescue mission successfully. The dead reckoning (DR) approach using self-contained sensors including an encoder, a gyroscope, and a magnetometer is one of the candidates, but position errors are accumulated as time passes. Therefore, the wireless positioning approach has been typically used as an alternative.

N. Efatmaneshnik and others [8] proposed a cooperative positioning system (CPS) for automobiles based on ranging and range-rate measurements from a vehicular ad hoc network, and R. Parker and others [9] proposed CPS for vehicles utilizing the received signal strength indicator (RSSI). However, since the position accuracy in the above methods is poor, it is hard to apply them to cooperative multi-robot systems. R. Kurazume and S. Hirose [10] developed CPS for robots using the angle of arrival (AoA). However, an array antenna for AoA should be installed at a fixed point with a fixed direction; thus, it is inadequate for localizing multiple mobile robots in unstructured dynamic environments, such as disaster areas.

This paper proposes the new collective intelligence network management architecture (CINeMA) of multiple mobile robots supporting seamless network connectivity and cooperative localization. The proposed architecture includes a resource manager that activates the robots so they do not disconnect from the network link by considering the RSSI and Link Quality Indicator (LQI). The robots are then driven to move around inside the safety region, maintaining global link connectivity even during a local connection failure.

The location manager in the architecture supports localizing robots by finding their relative locations as they move from a global outdoor environment to a local indoor position. The location manager uses a CPS based on the two-way ranging (TWR) technique. In the proposed TWR-based CPS, each non-localized mobile robot finds its position using bilateral range measurements of the nearby localized mobile robot. By employing a chirp spread spectrum ultra-wideband modulation technique, TWR measurements with an accuracy of less than 1 m can be achieved. The localized mobile robots with a GPS act as anchors and support the localization of mobile robots in the GPS-shadow region, such as in an indoor environment.

The rest of this paper is organized as follows. A collective intelligent robot system (CIRoS) architecture is given in Section II. In Section III, a radio map-based seamless routing scheme is introduced. Section IV describes the TWR-based

localization scheme. In Section V, the seamless routing and cooperative localization schemes are validated through numerical simulations, and Section VI describes their application to a search and rescue robot team. Finally, Section VII provides some concluding remarks.

II. CIRoS System Architecture

Generally speaking, multiple mobile robots cooperate together to achieve a common goal in a collective intelligent way, while sharing a common workspace. The overall goal-archiving software for collective intelligence typically handles a vast amount of functional data; thus, it requires several levels of software components to be combined, such as the behavior level, task level, and service level. We propose a layered software architecture that manages collective intelligent data, called CIRoS architecture, as shown in Fig. 1.

At the bottom of Fig. 1, the hardware abstraction layer and standard robot infrastructure layer construct the basic software framework of robots represented by Open Platform Robotic Services (OPRoS) [11]. The Collective Intelligence Network Management Layer supports a dynamic ad hoc mesh network configuration and efficient management under the conditions and information of the corresponding network. The Collective Intelligence Service Management Layer manages the goal-achieving process and allocates tasks to provide collective intelligence services such as remote operation, maintenance, formation control, and fault prediction. Here, we describe the Collective Intelligence Network Management Layer in more detail.

Collective intelligence network management layer. A collective intelligence network uses various kinds of networks such as WPAN and WLAN. In addition, there are many clusters, each of which corresponds to various robot teams. Thus, a special middleware that can integrate them is necessary. We suggest a middleware called CINeMA, which supports a dynamic ad hoc mesh network configuration and efficient management under the conditions and information of the corresponding network. CINeMA consists of a network configuration manager (NCM) to configure the total network system; a location manager (LM) to acquire and control the positions based on networks; a topology manager (TM) to manage the routing table; a traffic manager (TRM) to monitor the network traffic; and a resource manager (RM) to manage the resources of the network, predict network failures, and generate a redundancy path for the fault tolerance of the link, as shown in Fig. 2.

III. Radio Map-Based Seamless Routing Scheme

The RM in CINeMA is intended for a cooperative routing

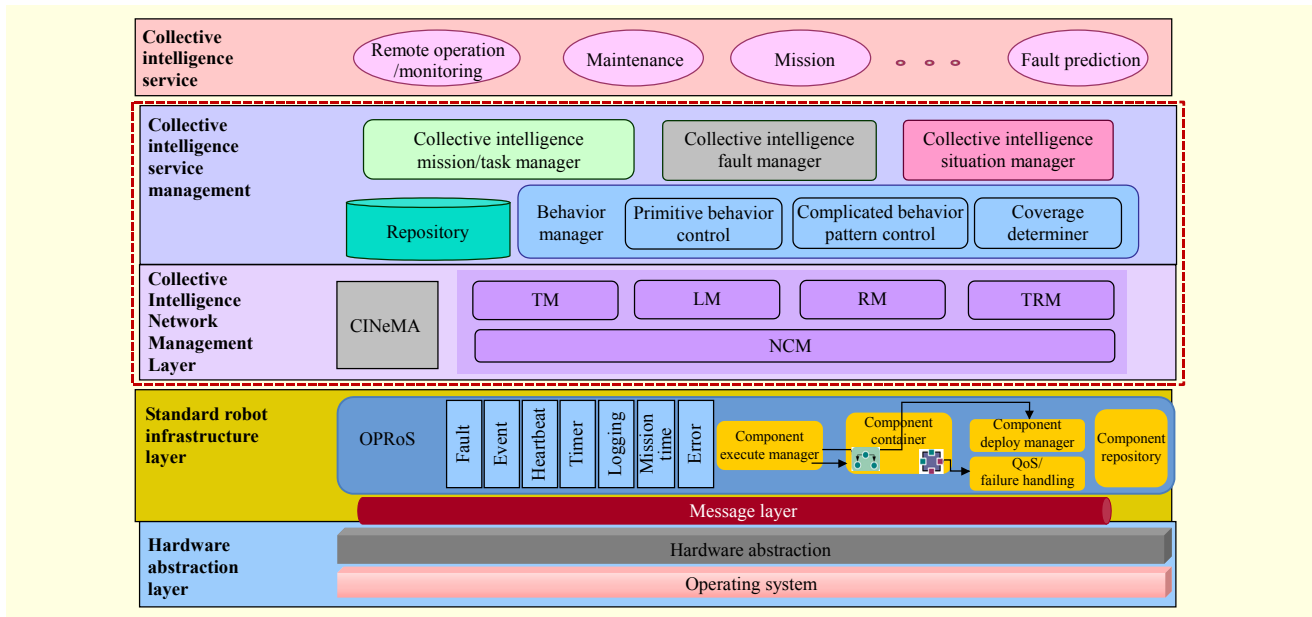


Fig. 1. CIRoS architecture: area within the dotted red line indicates key layers for collective intelligence functions.

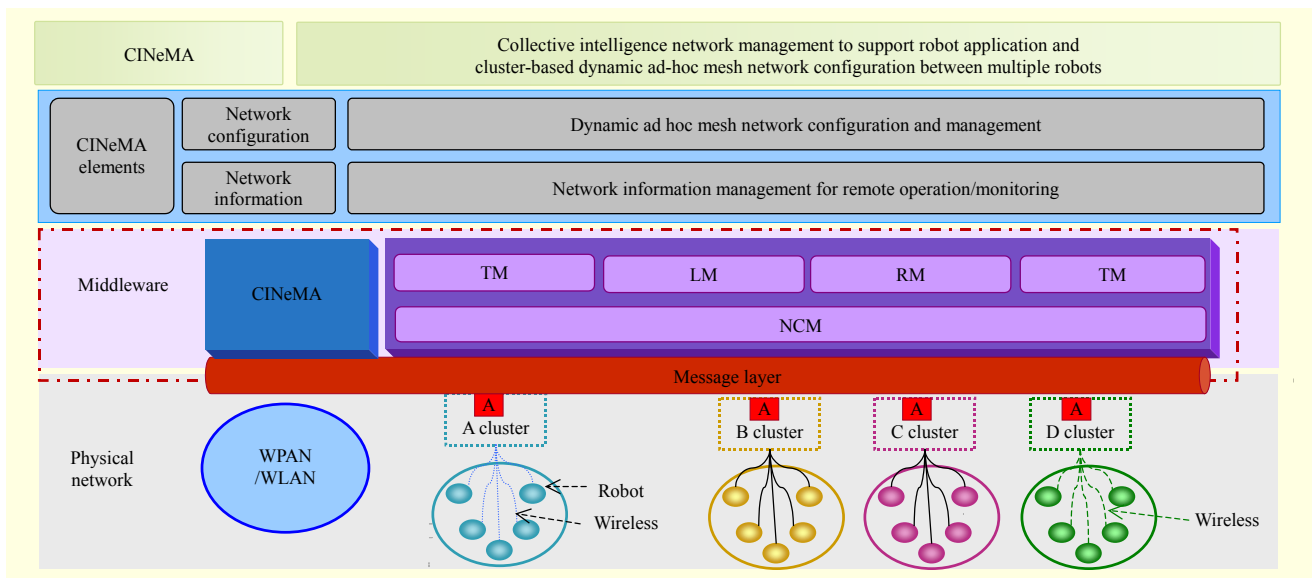


Fig. 2. Components of CINeMA.

robot system (CRRS) that maintains the network connectivity from the operation station to the front-end working robot. This system behaves as an autonomous reactive mobile router where robots dynamically move in response to the strength of the networking signal and the quality of the link among the cooperative robots. The algorithm used to establish a seamless global communication is composed of two steps. In the first step, the communication links are monitored and a network disconnection is predicted by analyzing the RSSI and LQI among the cooperative robots. Then, in the second step, the robots are driven to move around the safety region maintaining

the global link connectivity by using a virtual force model assisted by the extended Kalman filter (EKF) [12] and k -Nearest Neighborhood (k -NN) methods [13], even in the case of a local connection failure.

1. CRRS

In CRRS, a link path from the remote operator station to the front-end robot is established through cooperation of multiple mobile robots even in an environment where a network infrastructure is absent or damaged. To accomplish a given

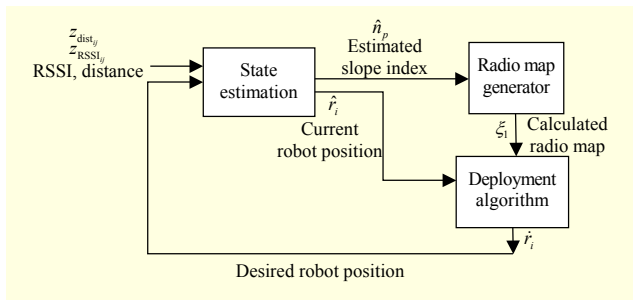


Fig. 3. CRRS process.

mission successfully, the routing robot team working as an autonomous reactive mobile router should maintain the quality of the communication link to assure seamless network connectivity. The whole process of the CRRS is composed of the following steps. In the first step, the CRRS must periodically monitor the communication links and estimate the robot positions and radio environment factors. Then, in the second step, the CRRS generates a radio map to predict a network disconnection by analyzing the RSSI and LQI among the cooperative robots. Finally, the robots are driven to move around the safety region using a deployment algorithm to maintain the global network connectivity. The whole process of the CSSR is shown in Fig. 3.

2. Network-Connection Model

To predict a network disconnection, we propose a network-connection model on the basis of the RSSI and LQI among cooperative routing robots, as shown in Fig. 4. The network-connection area is classified into the following four regions according to the RSSI value of the robot: close, safe, monitoring, and emergency. Network connectivity is assured when one of the other routing robots exists inside a close or safe region. When any robot inside of a safe region moves to the monitoring region, its location is allocated by the deployment algorithm to maximize the network connectivity. When any robot is absent inside the monitoring region but a robot is in the emergency region, the RM notifies a disconnection alarm to the robots and operator.

LQI implies the quality measurement of a received packet, and has a value in the range of decimal zero to 255. The IEEE 802.15.4 standard requires that the desired packet error rate be 1% or less to communicate between nodes. To satisfy this requirement, the minimum LQI threshold is 100 [14]. Therefore, if the value of LQI is under 100, then the area is remodeled as the emergency region. When LQI is low and RSSI is high, the area is remodeled as the monitoring region to avoid obstacles because this state indicates that there are obstacles near the robot.

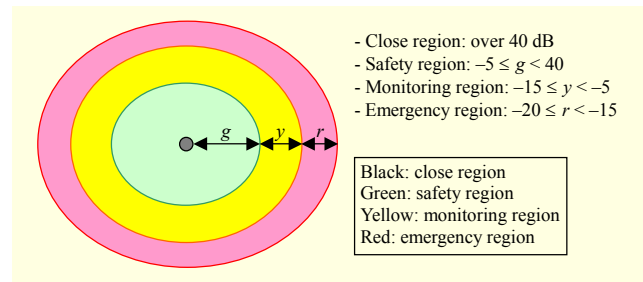


Fig. 4. Network-connection model based on RSSI.

Table 1. Slope indexes in log-distance path loss model.

Environment	Slope index (n)
Free space	2
Urban area	2.7-3.5
Shadowed urban area	3-5
Indoor LOS (line of sight)	1.6-1.8
Indoor no LOS	4-6

3. Estimation of Radio Environment

To predict the possible area where a robot with an explore mode can move freely, the radio map generated by multiple robots should be estimated. The estimation process is described as follows:

- 1) Propagation model: a propagation model represents the log-distance path loss model in a radio environment.

$$P_{dBm} = L_0 + 10n \log\left(\frac{\|r_i - r_j\|}{d_0}\right) + \epsilon, \quad (1)$$

where L_0 is the measured loss power at 1 m between robots, r_i is the position of the i th robot, r_j is the position of the j th robot, d_0 is a reference distance (1 m), n is the slope index, and ϵ is drawn from a Rayleigh or Rician distribution. Generally, the slope index grows bigger in the obstacle environment, as shown in Table 1.

- 2) Slope index estimation: state variables in the radio-propagation dynamic system are composed of the positions, velocities, and slope indexes of robots. The system dynamics and state vector are represented by the following equations.

$$\mathbf{x}_{k+1} = A\mathbf{x}_k + w_k, \quad (2)$$

$$\mathbf{x} = \left[r_{xi}, \mathbf{v}_{xi}, r_{yi}, \mathbf{v}_{yi}, r_{xj}, \mathbf{v}_{xj}, r_{yj}, \mathbf{v}_{yj}, n \right]^T,$$

where \mathbf{v} is the velocity of each robot, w_k is white Gaussian noise, \mathbf{x}_k is the state vector at time k , and A is a state transition matrix. From the system dynamics given in (2), the system measurement function is modeled with the relative distance and RSSI between robots, and is represented as follows:

$$z_k = \mathbf{h}(\mathbf{x}_k) + v_k$$

$$z = \begin{bmatrix} z_{\text{dist}} \\ z_{\text{RSSI}} \end{bmatrix} = \begin{bmatrix} \|r_i - r_j\| \\ L_0 + 10n \log(\|r_i - r_j\|) \end{bmatrix} + \begin{bmatrix} v_1 \\ v_2 \end{bmatrix}, \quad (3)$$

where $\mathbf{h}(\cdot)$ is the nonlinear vector of the measurement, v_k is white Gaussian noise, $\|\cdot\|$ is the Euclidean distance between robots, n is the slope index, and L_0 is the measured loss power at 1 m between robots. To measure the relative distance and RSSI, we adapted the EKF process on the basis of the nonlinear characteristics. The designed EKF process is conducted in each of the neighboring robots.

3) Radio map generation and deployment: after the EKF process, the CRRS generates a radio map to predict a network disconnection by analyzing RSSI and LQI among the cooperative robots. For this, we propose a radio map generation method on the basis of a nonparametric estimation approach for the density estimation of the radio environment in disaster areas, which is called the k -NN method. The whole process of the radio map generation is composed of the following steps. In the first step, a grid point of the radio map finds the nearest robot among cooperative robots by measuring the shortest distance between the grid point and robots. Then, that grid point of the map is assigned to the same slope index of the nearest robot, as shown in (4). In the second step, the radio map is generated by integrating the estimated RSSI value of all grid points, as shown in (5).

$$r_{\min} = \operatorname{argmin}_{p \in \text{MAP}} \{d(p, r_i)\}, \quad (4)$$

$$\hat{n}_p = \gamma(r_{\min}),$$

$$\xi_1 = \widehat{\text{RSSI}}_p$$

$$= L_0 + 10\hat{n}_p \log(\|p - r_i\| / d_0) - \text{OFFSET}, \quad (5)$$

where p is each grid position on the radio map, r_i is the position of the robot, and $d(\cdot)$ is the distance between the grid position and the robot. In addition, $\gamma(\cdot)$ is the function for selecting the slope index at position p , and OFFSET is a system parameter, which has a constant value.

Finally, the robots are driven to move around the safety region using a deployment algorithm to maintain the global network connectivity. The robots are aware of the region they belong to and change their task accordingly. The virtual force model-based deployment algorithm between the region and action mode is as follows:

$$F_{ij}(i) = \begin{cases} -1 / d_{\text{based_rssij}} \times ((\mathbf{v}_j - \mathbf{v}_i) / d_{\text{based_rssij}}) & \text{Close region,} \\ 0 & \text{Safety region,} \\ (d_{\text{based_rssij}} - d_{\text{based_MAXrssij}}) \times ((\mathbf{v}_j - \mathbf{v}_i) / d_{\text{based_rssij}}) & \text{Monitoring region,} \\ \text{MAXDIST} \times ((\mathbf{v}_j - \mathbf{v}_i) / d_{\text{based_rssij}}) & \text{Emergency region,} \end{cases} \quad (6)$$

where $d_{\text{based_rssij}}$ is the distance between the i th and j th robots calculated from RSSI, as shown in (7).

$$d_{\text{based_rssij}} = \lambda / 4\pi \times 10^{L/10n}, \quad (7)$$

where λ is the wavelength of the signal, L is the path loss, and n is a slope index of the path loss. In (6), the distance between the i th and j th robots using the location sensor is represented by $d_{\text{based_distij}}$; the minimum distance between robots without a collision by $d_{\text{based_MAXrssij}}$; a position vector of a robot by \mathbf{v} ; and the practicable distance during one term by MAXDIST .

The calculated F_{ij} is used to determine the positions of the cooperative robots as follows:

$$\mathbf{v}_i = \mathbf{v}_{i-1} + \sum_j F_{ij} \times \text{MAXDIST}. \quad (8)$$

When the signal strength among robots is too strong, the negative force input commands the robot in the nearby region to avoid a collision with other robots. On the other hand, in the case where the signal strength is too weak, the positive force input commands the robot to follow the other robots.

IV. TWR-Based CPS

The location manager in the CINeMA supports localizing robots by finding their relative locations while moving them from a global outdoor environment into a local indoor position. The location manager uses a CPS based on the TWR technique. In the proposed TWR-based CPS, each non-localized mobile robot finds its position using the bilateral range measurements of the nearby localized mobile robot.

The process to establish a seamless global positioning is composed of the following steps. In the first step, the operation mechanism of the TWR-based CPS is introduced. Then, in the second step, the performance of the TWR-based CPS is enhanced by suggesting the position quality indicator, which represents the position accuracy for minimizing the accumulated position error, and the formation control protocol for maintaining a good geometry that improves the position accuracy.

1. Cooperative Positioning Robot System

The TWR-based CPS consists of a base station and mobile nodes, which are tags or anchors. The base station initiates and coordinates the network and sends anchor lists to the available tag. If the tag receives a start command, then it measures the TWR with anchors in the anchor lists and returns the measurements, such as the position and distance to the base station. The anchor is located in the known position and responds with a message received from the tags. The benefit of TWR-based CPS is that this system can maintain a good geometry using a few robots located in the known position.

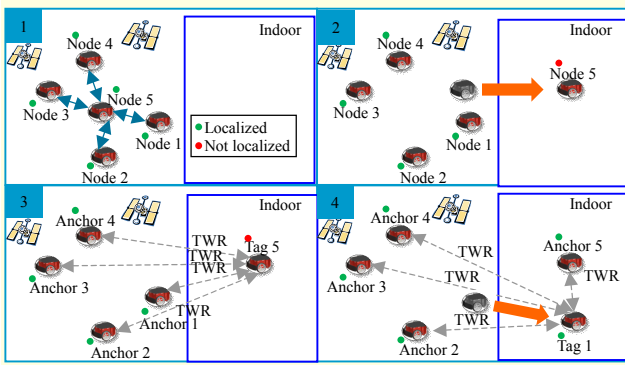


Fig. 5. Operational mechanism of TWR-based CPS.

Assume that some robots located in an outdoor area know their positions using a GPS and each of the robots moves forward into the indoor area. Then, the base station sets these as anchors and drives them so they do not move. Some robots that call a tag then move forward into an indoor area and acquire their positions from the anchor. In the next turn, the tags and anchors in an indoor area exchange their role inversely. Iterating these processes, the proposed TWR-based CPS localizes their positions, whereas the robots are moved from a global outdoor position into a local indoor position, as shown in Fig. 5.

2. Error Propagation and Location Propagation Indicator

As a tag localizes its position with anchors, the position error of the anchor propagates to the tag, and the position error of the tag accumulates the position errors of the anchor. To minimize the effect of error propagation, the location propagation indicator (LPI) enables the TWR-based CPS to select the best anchor lists for improving the position accuracy of the tag. To analyze the characteristics of the error propagation, the position error covariance of the tag, which represents the error density in the three-dimensional plane, is derived from the geometrical placement and position error covariance of the anchors. Assuming the three-dimensional position error vector (which consists of x , y , and z axes) of the i th anchor to be \mathbf{w}_i , the position covariance matrix of the i th anchor, ρ_i , is $E[\mathbf{w}_i \cdot \mathbf{w}_i^T]$, where $E[\cdot]$ is the expectation operator. Figure 6 shows a scenario in which the tag localizes its position from the anchors localized by a GPS. The position error propagation increases in proportion to the inner product of the directional cosine vector and the position error vector of the anchor. Directional cosine vector \mathbf{h}_i is the vector whose direction is from the anchor to the tag, and its norm is unity.

To formulate the position error propagation in TWR-based CPS, the ranging error, which represents the distance error density propagation $\mathbf{h}_i^T \mathbf{w}_i$, is visualized in Fig. 7.

A tag performs TWR with other anchors. Since the position

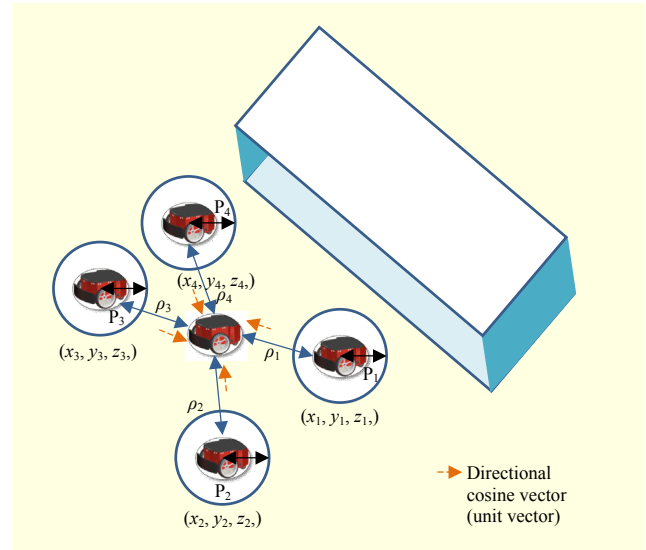


Fig. 6. Location error propagation of a mobile node.

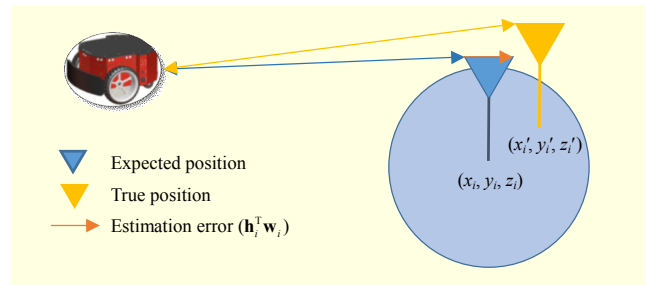


Fig. 7. Range error propagation of a mobile node.

error of the anchor is not zero, the ranging error increases because of an imperfect system model, which means that the acquired ranging measurement differs from the nominal distance between the tag and the estimated position of the anchor. This difference is given by the inner product of the directional cosine vector \mathbf{h}_i between the tag and i th anchor. In addition, \mathbf{h}_i from the i th anchor is written as

$$\mathbf{h}_i = \begin{bmatrix} -\frac{x_i - x}{r_i} \\ -\frac{y_i - y}{r_i} \\ -\frac{z_i - z}{r_i} \end{bmatrix}^T, \quad (9)$$

where x , y , and z are the positions of the tag; x_i , y_i , and z_i are the positions of the i th anchor acquired from a GPS, and $r_i = \sqrt{(x - x_i)^2 + (y - y_i)^2 + (z - z_i)^2}$. A TWR measurement that represents the relative distance between the tag and i th anchor is then represented as follows:

$$\rho_i = \sqrt{(x - x_i)^2 + (y - y_i)^2 + (z - z_i)^2} + \mathbf{h}_i^T \mathbf{w}_i + v_i, \quad (10)$$

where v_i is the measurement noise with variance σ^2 . The covariance between the i th and j th range measurements, which means the relative power of the noise, is calculated as below:

$$\begin{aligned}
\text{cov}(\mathbf{h}_i^T \mathbf{w}_i + v_i) &= E\left\{\left(\mathbf{h}_i^T \mathbf{w}_i + v_i\right)\left(\mathbf{h}_j^T \mathbf{w}_j + v_j\right)\right\} \\
&= E\left\{\mathbf{h}_i^T \mathbf{w}_i \mathbf{w}_j^T \mathbf{h}_j^T + \mathbf{h}_i^T \mathbf{w}_i v_j + v_i \mathbf{h}_j^T \mathbf{w}_j + v_i v_j\right\} \\
&= \mathbf{h}_i^T P_i \mathbf{h}_j^T + \sigma^2 (i = j) \\
&= 0 (i \neq j).
\end{aligned} \tag{11}$$

Using this information, and assuming the errors of the ranging measurement are independent and identically distributed, the covariance matrix of the N th ranging measurement is derived as follows:

$$\begin{aligned}
Q &= \begin{bmatrix} \mathbf{h}_1^T P_1 \mathbf{h}_1 + \sigma^2 & 0 & \cdots & 0 \\ 0 & \mathbf{h}_2^T P_2 \mathbf{h}_2 + \sigma^2 & \cdots & 0 \\ \vdots & \vdots & \ddots & \vdots \\ 0 & 0 & \cdots & \mathbf{h}_N^T P_N \mathbf{h}_N + \sigma^2 \end{bmatrix} \\
&= \begin{bmatrix} \mathbf{h}_1^T P_1 \mathbf{h}_1 & 0 & \cdots & 0 \\ 0 & \mathbf{h}_2^T P_2 \mathbf{h}_2 & \cdots & 0 \\ \vdots & \vdots & \ddots & \vdots \\ 0 & 0 & \cdots & \mathbf{h}_N^T P_N \mathbf{h}_N \end{bmatrix} + \sigma^2 I_N,
\end{aligned} \tag{12}$$

where I_N is an identity matrix of dimension N by N . The location of the tag is acquired from the following formula:

$$\Delta \mathbf{x} = (H^T Q^{-1} H)^{-1} H^T Q^{-1} \Delta \mathbf{r}. \tag{13}$$

In this case, the location covariance matrix is calculated as

$$\begin{aligned}
\gamma &= \text{cov}(\Delta \mathbf{x}) \\
&= (H^T Q^{-1} H)^{-1} H^T Q^{-1} \text{cov}(\Delta \mathbf{r}) Q \left\{ Q^{-1} H^T (H^T Q^{-1} H)^{-1} \right\}^T \\
&= (H^T Q^{-1} H)^{-1}.
\end{aligned} \tag{14}$$

In succession, since the position of the tag is known, this terminal can be changed into an anchor with position covariance γ_1 . In this case, assume that another tag enters further indoor than the previous tag. The tag can then be localized through TWR. The ranging covariance of this system can be written as

$$Q = \begin{bmatrix} \mathbf{h}_1^T \gamma_1 \mathbf{h}_1 & 0 & \cdots & 0 \\ 0 & \mathbf{h}_2^T P_2 \mathbf{h}_2 & \cdots & 0 \\ \vdots & \vdots & \ddots & \vdots \\ 0 & 0 & \cdots & \mathbf{h}_N^T P_N \mathbf{h}_N \end{bmatrix} + \sigma^2 I_N. \tag{15}$$

To explain the quantity of the error propagation, the location error propagation matrix is a necessary and sufficient condition and can be derived from the ranging error propagation matrix Q . On the other hand, this indicator complicates the calculations, as it needs all covariance matrices from the anchors that are involved in the localization. For this reason, this method will be impractical in a real system.

Therefore, this paper suggests the use of an LPI. If the mobile node localizes its position using GPS, then the LPI is zero. In addition, if the location is calculated from other

anchors, then its LPI is one more than the maximum of the LPI values of the anchor used for positioning. This simple indicator shows that the greater LPI means a greater probability of having a large location covariance matrix. LPI is calculated simply, while less information is given compared to the location covariance matrix. On the other hand, the system using LPI works well in real applications. The position accuracy is enhanced using measurements from a low LPI or by not using measurements from a high LPI.

In the TWR-based CPS, the tag calculates its position with fixed anchors. If a tag has to move out of the workspace, then the location error grows more as the tag moves farther. In general, the root mean square (RMS) error of the tag position is a convex curve, which means that the RMS error increases faster as the tag moves out of the workspace as compared with a linear increase. This implies that if the final destination is far from the workspace, then moving directly to the goal is not the best scenario for the TWR-based CPS. This is verified in Section V.

V. Simulation Results

In this paragraph, the seamless routing and cooperative localization schemes are validated through numerical simulations. In the first section, the seamless radio map-based routing scheme is verified by analyzing its performance based on the comparison results of the conventional approach, which in turn is based on the distances between multiple robots. In the following section, two moving scenarios for TWR-based CPS are compared in terms of the final location error.

1. Simulation for Radio Map-Based Seamless Routing Scheme

The results of the conventional approach, which is based on the distances between multiple robots, are compared to those of the proposed approach in a computer simulation. The simulation results of the suggested network-connection model using the RSSI in a multi-robot system are illustrated with connectivity among the robots. A front-end tank robot (TBOT) randomly moves, and another robot is driven by each approach. The results are shown in Fig. 8.

As shown in Fig. 8(a), a routing robot seems to follow the TBOT at regular intervals in all approaches, but in reality, it does not. If the strength is under -20 dB, then the network for communication is regarded as a disconnection. In Fig. 8(b), the network was disconnected in the conventional approach based on distance. Furthermore, the disconnection increased with the slope index, which reflected the level of the multipath environment. In a multipath environment, the distance-based approach is not stable. On the other hand, our proposed approach provides a reliable network, because the robot

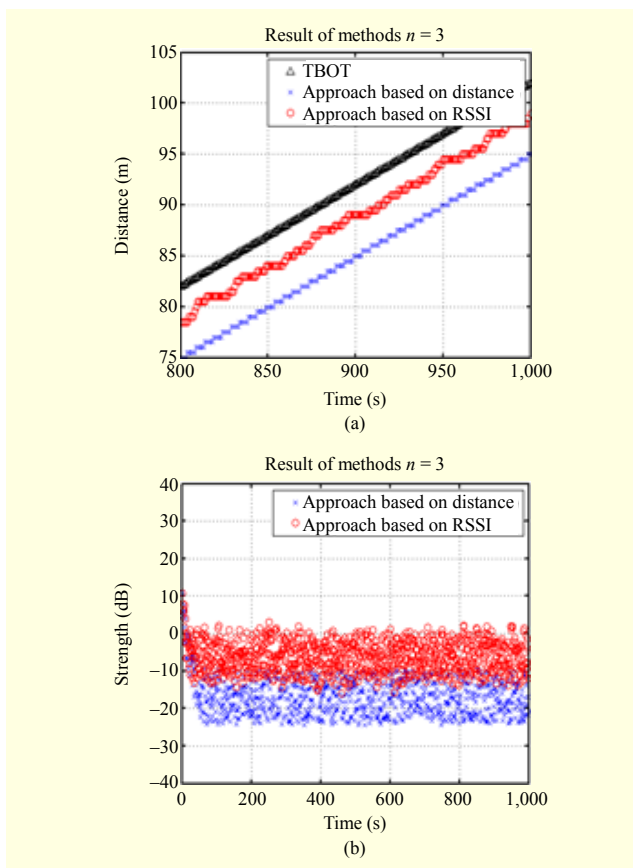


Fig. 8. Simulation results: (a) result of estimate distance and (b) RSSI result between robots after each approach is applied.

previously moves inside a safety region when it predicts a disconnection of the network.

2. Simulation for TWR-Based CPS Scheme

The location error in the final destination in TWR-based CPS is influenced by the way the formation control is conducted. Figure 9 shows several types of formation controls of the anchors and tags. In scenario 1, node 5 moves directly to the final destination. In scenario 2, the positions of tags 6 and 7 are calculated, and tag 5 then localizes with the ranging measurements from mobile nodes 1, 2, 6, and 7.

The tag position and anchor geometry have an effect on the location error of the tag. On the other hand, the error density for the tag increases nonlinearly. In the initial state, the workspaces of scenarios 1 and 2 are equal. On the other hand, scenario 2 moves mobile nodes 6 and 7 to move the anchor geometry. A comparison of scenarios 1 and 2-2 clearly show that scenario 1 will cause twice the errors than scenario 2-2. On the other hand, error propagations are caused by mobile nodes 6 and 7 in scenario 2-1. If the error propagations from mobile nodes 6 and 7 are small, then scenario 2 will show a smaller number of

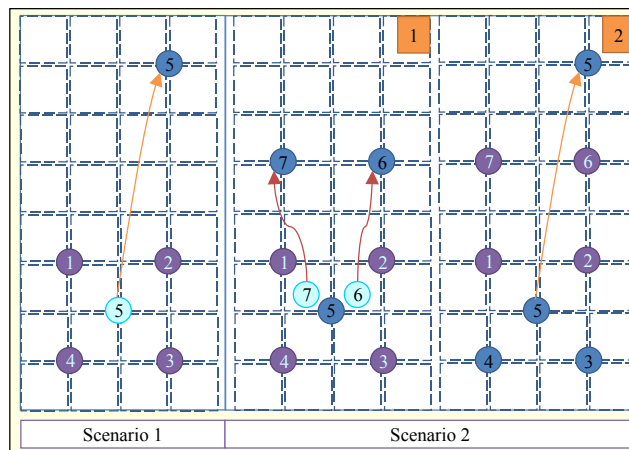


Fig. 9. Scenario of two TWR-based CPSs.

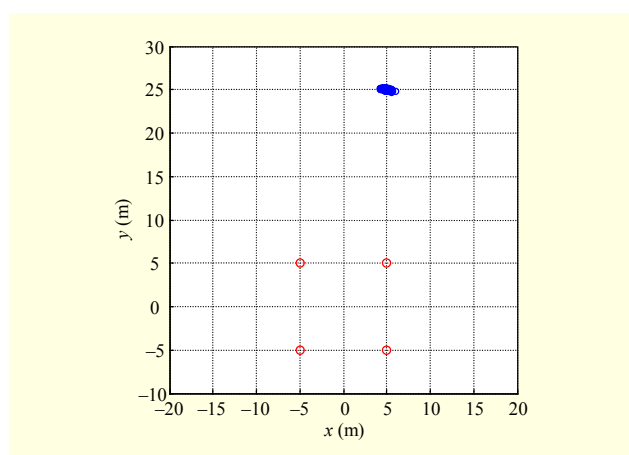


Fig. 10. Simulation results for scenario 1 (moving the tag only).

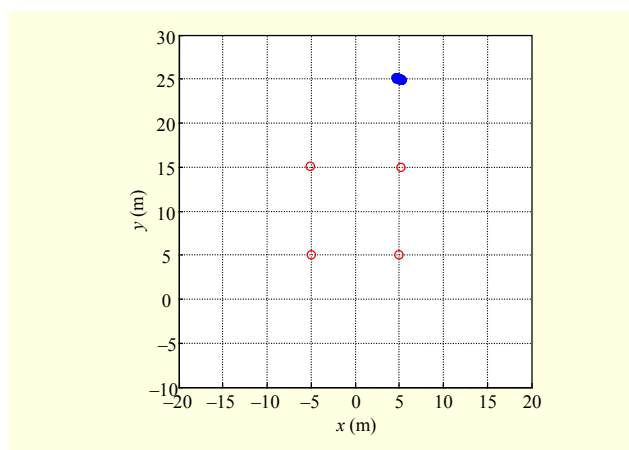


Fig. 11. Simulation results for scenario 2 (moving the tag and workspace together).

position errors.

We assume that the measurement distance error is 0.1 m because of UWB resolution, and the simulation was repeated 90,000 times. Figures 10 and 11 show that in scenario 1, the

standard deviation of the location error is 0.25 m, and in scenario 2, the standard deviation of the location error is 0.16 m. These results imply that the position accuracy of a tag is improved if both the tag and the workspace move together. TWR-based CPS could modify the positions of anchors by mode change. Therefore, this paper shows that our proposed TWR-based CPS mitigates the tag-position error by 36% when compared to conventional TWR-based systems.

VI. Integration of Search and Rescue Robot Team

For a practical mobile robot team carrying out a search and rescue mission in a disaster area, two missions were allocated by CINEMA as follows. The first mission is to search for the object/human target through a tele-operation of the front-end robot, which includes a camera; and the second mission is to maintain seamless network connectivity through autonomous reactive mobile routers, which consist of a laser range finder (LRF), a laptop, and a network board. The LRF is used to avoid obstacles, and our CINEMA middleware is operated on the laptop. The network board consists of WLAN and WPAN (ZigBee and UWB) modules. The WPAN module is used to find the route to the communication link, and WLAN is used to transfer high-capacity data, such as a video stream. The experimental setup is shown in Fig. 12. The map was generated by robots using simultaneous localization and mapping in advance. The size is approximately 80 m × 30 m. Two experiments were conducted and are explained as follows:

- Test I: confirm the tele-operation between a human (ROC) and front-end robot, as shown in Fig. 12(a). The exploration robot moves to the position of the red flag from the initial position near the ROC, and continuously transmits the captured video to the ROC. Other robots connect the human with the exploration robot. The routing robots relay the data and estimate the radio environment to predict a network disconnection between the human and robot.
- Test II: confirm cooperative radio map generation (see Fig. 14(b)). There are obstacles and a wall between the robots. The robots generate a radio map to find the area in which communication is possible.

The results of Test I show that the exploring robot was continuously tele-operated from the ROC, which acquired a remote video and the positions of the robots. When the robots predicted the disconnection of the network, the robot notified the ROC and other robots of the warning. The user could control the robot and confirm the state of the network. The results of the experiment are shown in Fig. 13.

The ROC displays the remote video and positions, as can be seen in Fig. 13(a). The red circle in Fig. 13(b) indicates that the network connection between robots was considerably poor and

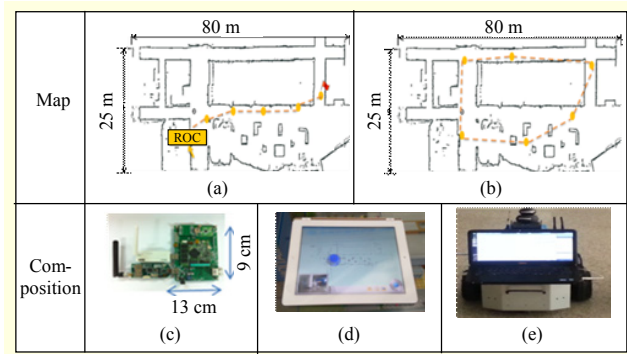


Fig. 12. Experimental composition: (a) Test I; (b) Test II; (c) network board consisting of WLAN and WPAN module; (d) remote operator center (ROC) acquiring the video stream and controlling the remote multi-robots; and (e) routing robots autonomously moving during moving mode.

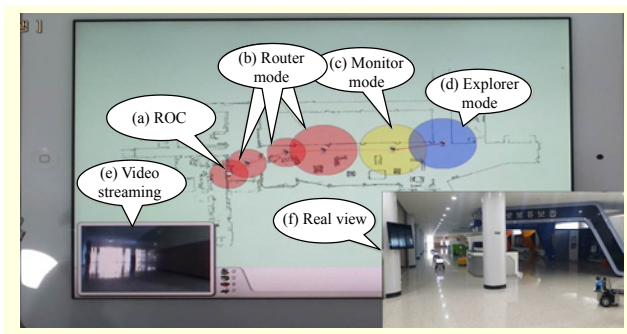


Fig. 13. Experimental results of Test I.

there were robots in the emergency region. The robots changed into the router and simply relayed the data between the ROC and the exploring robot. The yellow circle in Fig. 13(c) is the monitor mode. The robot did not move because the radio signal changed rapidly because of moving the exploring robot. The blue circle in Fig. 13(d) means that it was possible to communicate with other robots within the specific region, and the robot was in explorer mode. The sizes of the circles were different because the radio environment was different.

The estimated states of the radio environment are reflected in Fig. 14. This figure shows the results of Test II. In the experiment, the six robots were placed as shown in Fig. 14(a). The robots sent and received a radio signal to each other. The result of Fig. 14(d) is the map generated by each robot. They simply show the local coverage and those robots that are able to communicate. As an example, Fig. 14(d-iv) shows that robot 4 can communicate with the nearest-right and nearest-left robots. The regions of the black boxes indicate that the communication is impossible, and there are obstacles or walls in the area. Figure 14(b) shows that the result of using previous approaches is simply the sum of the coverage of the individual

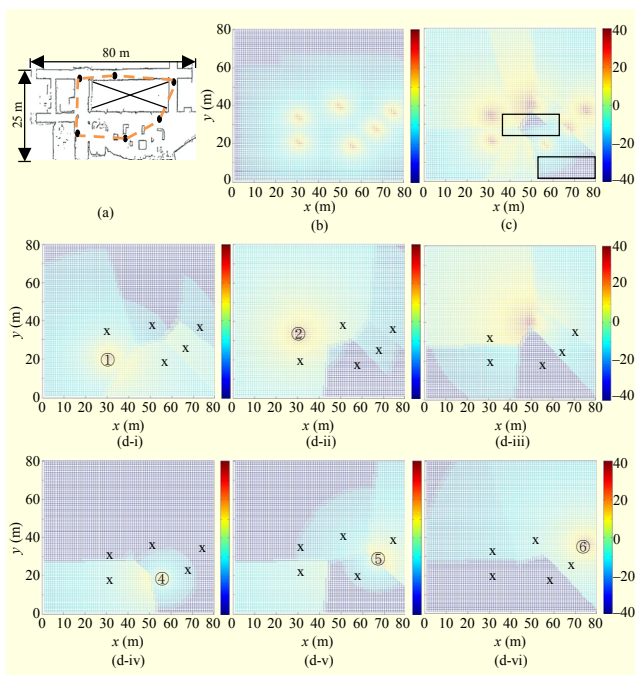


Fig. 14. Experimental results of Test II: (a) real map with wall and obstacle; (b) radio map using a previous method; and (c) a map using our proposed method. Region of the black boxes is the disconnection area of the network. Map of (d) is generated by each robot of (1)–(6), and “x” is the position of another robot

robots, and that these previous approaches did not reflect useful information between the robots. Figure 14(c) shows our proposed multiple maps matched using k -NN. As a result, they can give the user a significant amount of information, including the global coverage of the communication and the approximate positions of the obstacles without specific sensors. As a result, the mean squared error of the estimated values is approximately 3 dB.

VII. Conclusion

For a practical mobile robot team carrying out a search and rescue mission in a disaster area, this paper introduced the new collective intelligence network management architecture (CINeMA) for multiple mobile robots supporting seamless network connectivity and cooperative localization. The proposed architecture supports a radio map-based seamless routing scheme that makes the robots move around a safe region while maintaining global link connectivity by predicting both the strength of the networking signal and the quality of links among the cooperative robots. It also provides a TWR-based CPS scheme that makes the non-localized mobile robot find its position using a two-way range technique to the localized mobile robot nearby while moving multiple robots

from the good Global Positioning System (GPS) region, such as an outdoor environment, to a GPS-shadow region, such as an indoor environment. The proposed seamless routing and cooperative localization schemes were validated through numerical simulations. As a result, CINeMA helps multiple cooperative robots conduct a search and rescue mission successfully even in an environment in which the network infrastructure is destroyed or a GPS is unavailable. In addition, it provides network resource information such as the radio environment map and approximate positions of the obstacles and robots without specific infra-structure sensors.

References

- [1] J. Fink, A. Ribeiro, and V. Kumar, “Robust Control of Mobility and Communications in Autonomous Robot Teams,” *IEEE Access*, vol. 1, May 2013, pp. 290–309.
- [2] J. Fink and V. Kumar, “Online Methods for Radio Signal Mapping with Mobile Robots,” *IEEE Int. Conf. Robot. Autom.*, Anchorage, AK, USA, May 3–7, 2010, pp. 1940–1945.
- [3] M. McClure, D. Corbett, and D. Gage, “The DARPA LANDroids Program,” *Soc. Photographic Instrum. Eng.*, Orlando, FL, USA, vol. 7332, Apr. 2009.
- [4] L. Sabattini, N. Chopra, and C. Secchi, “Decentralized Connectivity Maintenance for Cooperative Control of Mobile Robotic Systems,” *Int. J. Robot. Res.*, vol. 32, no. 12, Oct. 2013, pp. 1411–1423.
- [5] S. Zickler and M. Veloso, “RSS-Based Localization and Tethering for Moving Robots in Unknown Environments,” *IEEE Int. Conf. Robot. Autom.*, Anchorage, AK, USA, May 3–7, 2010, pp. 5466–5471.
- [6] M.M. Zavlanos, M.B. Egerstedt, and G.J. Pappas, “Graph-Theoretic Connectivity Control of Mobile Robot Networks,” *Proc. IEEE*, vol. 99, no. 9, Sept. 2011, pp. 1525–1540.
- [7] N. Bezzo et al., “A Decentralized Connectivity Strategy for Mobile Router Swarms,” *World Congress Int. Federation Autom. Contr.*, Milano, Italy, Aug. 28–Sept. 2, 2011, pp. 4501–4506.
- [8] M. Efatmaneshnik et al., “A Cooperative Positioning Algorithm for DSRC Enabled Vehicular Networks,” *Archives Photogrammetry, Cartography Remote Sens.*, vol. 22, 2001, pp. 117–129.
- [9] R. Parker and S. Valaei, “Vehicular Node Localization Using Received-Signal-Strength Indicator,” *IEEE Trans. Veh. Technol.*, vol. 56, no. 6, Nov. 2007, pp. 3371–3380.
- [10] R. Kurazume and S. Hirose, “Study on Cooperative Positioning System – Optimum Moving Strategies for CPS-III,” *IEEE Int. Conf. Robot. Autom.*, Leuven, Belgium, May 16–20, 1998, pp. 2896–2903.
- [11] C. Jang et al., “OPRoS: A New Component-Based Robot Software Platform,” *ETRI J.*, vol. 32, no. 5, Oct. 2010, pp. 646–656.
- [12] H. Long et al., “Distributed Extended Kalman Filter Based on

Consensus Filter for Wireless Sensor Network,” *Intell. Contr. Autom.*, Beijing, China, July 6–8, 2012, pp. 4315–4319.

[13] C.M. Bishop, “*Pattern Recognition and Machine Learning*,” vol. 4, no. 4, New York, USA: Springer, 2006.

[14] Texas Instruments, *CC2520 DATASHEET*, 2007. Accessed Feb. 25, 2014. <http://www.ti.com/lit/ds/symlink/cc2520.pdf>



Chang-Eun Lee received his BS and MS degrees in electronics engineering from Hanyang University, Seoul, Rep. of Korea, in 1996 and 1998, respectively. He is currently working toward his PhD degree in information and communication engineering at Chungnam National University, Daejeon, Rep. of Korea.

From 1998 to 2000, he was a researcher at LG Industry System, Seoul, Rep. of Korea, where he worked on intelligent building automation systems. Since 2001, he has been with the Electronics and Telecommunications Research Institute, Daejeon, Rep. of Korea, where he has researched in the fields of intelligent robot control systems and home network systems. His research interests are artificial intelligence; robot software frameworks; and distributed and cooperative robot control.



Hyun-Ja Im received her BS and MS degrees in electronics engineering from Chungnam National University, Daejeon, Rep. of Korea, in 2007 and 2009, respectively. Since 2010, she has been with the Electronics and Telecommunications Research Institute, Daejeon, Rep. of Korea, where she has

researched in the field of intelligent robot control systems. Her research interests include cooperative robot control and embedded systems.



Jeong-Min Lim received his BS and MS degrees in information and communication engineering from Chungnam National University, Daejeon, Rep. of Korea, in 2011 and 2013, respectively. He is currently pursuing his PhD degree in information and communication engineering at Chungnam National University.

His research interests are cooperative positioning systems.



Young-Jo Cho received his BS degree in control engineering from Seoul National University, Rep. of Korea, in 1983 and his MS and PhD degrees in electrical engineering from KAIST, Seoul, Rep. of Korea, in 1985 and 1989, respectively. He joined the Electronics and Telecommunications Research Institute (ETRI), Daejeon, Rep. of

Korea, in 2004 as a vice president heading the Intelligent Robot Research Division. Before joining ETRI, he was a principal researcher at the Korea Institute of Science and Technology, Seoul, Rep. of Korea and director of the R&D center at iControls, Inc., Seoul, Rep. of Korea. He is now a principal member of the engineering staff at ETRI, and his primary research interest is in network-based intelligent robots.



Tae-Kyung Sung received his BS, MS, and PhD degrees in control and instrumentation engineering from Seoul National University, Rep. of Korea, in 1984, 1986, and 1992, respectively. After working at both the Institute for Advanced Engineering and Samsung Electronics Co., Seoul, Rep. of Korea, he joined Chungnam National

University, Daejeon, Rep. of Korea, where he is currently a professor of the department of information communications engineering. He participated in several research projects in the area of positioning and navigation systems. His research interests are GPS/GNSS, geo-location, UWB WPAN positioning, and location signal processing.